Communication

The Intricacies of Inflammatory Bowel Disease: A Preliminary Study of Redox Biology in Intestinal Organoids

Georg Csukovich [1],[†], Janina Huainig [1],[†], Selina Troester [2], Barbara Pratscher [1] and Iwan Anton Burgener [1],[*]

1   Small Animal Internal Medicine, Vetmeduni, 1210 Vienna, Austria; georg.csukovich@vetmeduni.ac.at (G.C.)
2   Institute for Medical Biochemistry, Vetmeduni, 1210 Vienna, Austria
*   Correspondence: iwan.burgener@vetmeduni.ac.at
†   These authors contributed equally to this work.

Abstract: We evaluated the redox status, precisely glutathione levels, which have a major impact in cellular detoxification and antioxidant defence in IBD-derived and healthy intestinal organoids. Therefore, we wanted to explore the differences in terms of their redox balance and mitochondrial fitness. To this end, we introduced a Grx1-roGFP2 construct into the organoids by lentiviral transduction before performing a stress assay by treating the organoids with hydrogen peroxide and examined the GSH/GSSG ratio using confocal imaging. Using ratio imaging, we could detect statistically significant differences between healthy and IBD-derived samples. To gain more insight, we also performed a GSH/GSSG assay, which directly measured glutathione levels. This analysis revealed that both organoid lines had higher levels of oxidized glutathione due to the stress treatment demonstrated by a lower GSH/GSSG ratio compared to the untreated control. Nevertheless, the results showed no significant difference between healthy and IBD-derived organoids. We further challenged organoids with hydrogen peroxide after incubation with MitoTracker® to see if mitochondrial fitness might be different in IBD-derived organoids. However, these results were also very comparable. In summary, our preliminary findings indicate that both organoid lines demonstrate a well-functioning system in terms of analysis but show no clear difference between healthy and IBD-derived samples.

Keywords: intestinal organoid; redox biology; IBD; glutathione; oxidative stress; ROS; redox imaging

1. Introduction

In vitro cultured organoids can model the physiological and morphological characteristics as well as cell signaling pathways within humans or animals. Gastrointestinal organoid cultures are most commonly derived from adult stem cells (ASC) that reside in the crypts of the gastrointestinal tract. The stem cells can be isolated from the tissue and retain their function and mutations from their residence site in the gut when maintained under defined cell culture conditions [1]. This important step allows us to create a model that imitates organ function, composition and development. Current research largely comprises the study of normal and pathological circumstances and their application to test possible therapeutics for different diseases [2,3].

One major affliction of the gut is inflammatory bowel disease (IBD), which leads to the infiltration of lymphocytes and macrophages, i.e., inflammation, and to general signs of gastrointestinal dysfunction like weight loss and diarrhea. Genetic and environmental changes have been implicated with the occurrence of IBD and lead to the overgrowth of pathogenic bacteria with the outcome of inflammation and intestinal injury. The exact underlying reasons that trigger this kind of disease are still not well understood [4,5]. However, interestingly many pet animals like dogs develop IBD spontaneously, while rodents like mice require an induction of IBD-like symptoms in order for them to serve as an IBD model [6]. Unlike humans, canine IBD is not classified into Crohn's disease and ulcerative colitis, but is rather a chronic disease diagnosed by the exclusion of common causes (e.g., tumors) and the histologic confirmation of the inflammation of the intestinal mucosa [7,8].

A critical factor contributing to IBD could be reactive oxygen species (ROS) [9,10]. Redox reactions are key functions for the whole mechanism to transport electrons from a donor to an acceptor molecule, and thus have an important role in various signaling processes within our bodies. Different types of ROS include hydrogen peroxide (H_2O_2), nitric oxide (NO), hydroxyl radicals (OH^-) and many more that are usually tightly controlled, but can oxidize lipids and proteins when they accumulate, and therefore harm the cell [11].

The two main sites for ROS production are the cytoplasm and the inner mitochondrial membrane. The formation of mitochondrial ROS (mtROS) happens under physiological respiratory conditions as a consequence of proton leakage and is detoxified by mitochondrial peroxiredoxins [12]. However, this process can be amplified due to cellular stress and high amounts of mtROS can cause the induction of mitophagy and apoptosis [13]. Since H_2O_2 originating from mitochondria can readily diffuse across cellular membranes, it can also be highly toxic to the entire cell if not eliminated immediately. This process is mainly carried out by glutathione, which can be found in its reduced form (i.e., GSH) and its oxidized form (i.e., GSSG) throughout the cell and in various organelles [14,15].

Usually, glutathione is present in larger quantities in its reduced form in healthy and balanced conditions. According to this information, the GSH/GSSG ratio can be used to determine the stress status of the cell, with low GSH/GSSG ratios indicating physiological conditions. If the cell is exhausted because of stress treatment, the oxidized form of glutathione accumulates and the GSH/GSSG ratio is higher. Therefore, the balance of reduced (GSH) and oxidized (GSSG) glutathione is essential for the maintenance of normal homeostasis [15,16]. If these conditions are skewed for whatever reason and the balance between ROS generation and elimination is tilted, the cell is undergoing so-called "redox stress".

The aim of this study was to investigate whether intestinal organoids derived from IBD patients are more sensitive to extrinsically induced redox stress and cannot withstand ROS as well as healthy organoids. Therefore, we analyzed the capability of canine intestinal organoids derived from healthy and IBD dogs to deal with redox stress induced by hydrogen peroxide by determining GSH/GSSG ratios derived from glutaredoxin-1-based redox imaging. In addition, we employed an assay, which directly measures the relative amounts of oxidized and total glutathione. We also considered mitochondria as a major source of intracellular ROS by staining active mitochondria with MitoTracker® to analyze whether IBD-derived organoids might show a mitochondrial defect and therefore produce extensively more ROS upon H_2O_2 challenge. Overall, we could not find any significant difference between healthy and IBD-derived organoids in terms of their redox balance. However, we successfully established a relevant model to analyze the redox system in intestinal organoids, with the potential to expand this system to live cell imaging in the future.

2. Materials and Methods

2.1. Cultivation of Intestinal Organoids

Canine intestinal crypts were isolated from duodenum according to Kramer et al., 2020 [17]. Canine IBD is mostly evident in the duodenum of affected dogs and histologic diagnosis is commonly based on duodenal biopsies. Based on the guidelines of the institutional ethics committee, the use of tissue material collected during therapeutic excision or post-mortem is included in the University's "owner's consent for treatment", which was signed by all patient owners. The growth medium consisted of 37% basal medium (Advanced DMEM/F12 supplemented with 2 mM GlutaMAX and 10 mM HEPES), $1 \times$ B27 (Invitrogen, ThermoFisher Scientific, Vienna, Austria), 1 mM N-Acetylcysteine (ThermoFisher Scientific, Vienna, Austria), 10 nM Gastrin (Sigma Aldrich, Vienna, Austria), 100 ng/mL Noggin, 500 nM A8301 (Bio-Techne Ltd., Minneapolis, MN, USA), 50 ng/mL HGF (PeproTech, Rocky Hill, NJ, USA), 100 ng/mL IGF1 (PeproTech, Rocky Hill, NJ, USA), 50 ng/mL FGF2 (PeproTech, Rocky Hill, NJ, USA), 10% (*v/v*) Rspondin1 and 50% (*v/v*) Wnt3a conditioned media. For the first two days of culture, 50 ng/mL mEGF (ThermoFisher Scientific, Vienna, Austria) and 10 μM Rock-inhibitor Y-27632 (Selleck Chemicals, Hous-

ton, TX, USA) were added. The growth medium was changed every two to three days. Weekly passaging at 1:4 to 1:8 split ratios was achieved by mechanical disruption using flame-polished Pasteur pipettes.

2.2. Immunofluorescent Analysis of Organoids

Organoids were fixed with 2% paraformaldehyde (PFA) for 15 min and stained according to a previously published protocol including a clearing step after organoid staining [18]. Organoids were stained with the 1:100 Claudin 7 Polyclonal Antibody (Invitrogen, ThermoFisher Scientific, Vienna, Austria) for tight junctions with the secondary antibody AF-488 goat anti-rabbit (Invitrogen, ThermoFisher Scientific, Vienna, Austria) diluted 1:500, 1:200 phalloidin (Alexa Fluor 647, Invitrogen, ThermoFisher Scientific, Vienna, Austria) to visualize actin filaments, and with 4 µg/mL 4′,6 diamino-2-phenylindole (DAPI; Sigma-Aldrich, Vienna, Austria) for nuclear staining. Confocal images were acquired using a Zeiss LSM 880 confocal microscope (Zeiss, Jena, Germany).

2.3. Production of Lentiviral Particles and Transduction of Organoids

In order to generate organoids expressing a redox-sensitive GFP, lentiviral particles carrying the Grx1-roGFP2 plasmid had to be produced and subsequently transduced into the respective organoids. pEIGW Grx1-roGFP2 was a gift from Tobias Dick (Addgene plasmid # 64990; http://n2t.net/addgene:64990, accessed on 8 August 2023; RRID:Addgene_64990).

On day one, the Lenti-X 293T cells (Takara bio, Saint-Germain-en-Laye, France) were split with trypsin and seeded in 10 cm2 dishes. The next day, 4 µg Grx1-roGFP2 plasmid and 2 µg psPAX2 and 1 µg pMD2.G packaging plasmids were mixed with 3 µL Polyethyleneimine HCI MAX (1 mg/mL; PEI; Polysciences Europe) per µg of DNA and incubated for 20 min at room temperature. psPAX2 was a gift from Didier Trono (Addgene plasmid # 12260; http://n2t.net/addgene:12260, acessed on 8 August 2023; RRID:Addgene_12260) and pMD2.G was a gift from Didier Trono (Addgene plasmid # 12259; http://n2t.net/addgene:12259, acessed on 8 August 2023; RRID:Addgene_12259). This transfection mix was added dropwise to Lenti-X 293T cells and incubated overnight. On the third day, the medium was changed to organoid transfection medium, which consisted of Advanced DMEM/F12 (Fisher Scientific), 1 × GlutaMAX (ThermoFisher Scientific, Vienna, Austria), 10 mM HEPES (ThermoFisher Scientific, Vienna, Austria), 1 × B27 (ThermoFisher Scientific, Vienna, Austria), 1 × N2 (ThermoFisher Scientific, Vienna, Austria), 1 mM N-Acetylcysteine (ThermoFisher Scientific, Vienna, Austria), 500 nM A8301 (Bio-Techne Ltd., Minneapolis, MN, USA), 10 µM SB202190 (Selleck Chemicals, Houston, TX, USA), 10 nM Gastrin (PeproTech, Rocky Hill, NJ, USA), 50 ng/mL HGF (PeproTech, Rocky Hill, NJ, USA), 50 ng/mL mEGF (ThermoFisher Scientific, Vienna, Austria), 100 ng/mL mNoggin (PeproTech, Rocky Hill, NJ, USA), 10 µM Y-27632 (Selleck Chemicals) and 5 µM CHIR99021 (Sigma-Aldrich, Vienna, Austria). On the following two days, the lentiviral particles were harvested by filtration through a 45 µm filter (qPORE) using a syringe. The virus supernatant was stored at 4 °C until further use.

For the transduction of the organoids, 1×10^6 cells of trypsinized organoids were seeded in 1.5 mL organoid transfection medium in a 6-well plate. To each well, 1.5 mL virus supernatant and 10 µg/mL Polybrene transfection reagent (Merck, Darmstadt, Germany) were added. The organoids were transfected via spinoculation, which was conducted for one hour at $600 \times$ g and subsequent incubation for three hours at 37 °C. After this step, the suspension was centrifuged at $300\times$ *g* for 5 min followed by two washing steps with DPBS. The cells were seeded in 24-well plates and after a few days sorted by Flow Cytometry (SRT, Beckman Coulter, Vienna, Austria) selecting for GFP positive cells to obtain a pure population of Grx1-roGFP2 expressing organoids.

2.4. Glutaredoxin-Based Redox Imaging

For redox imaging, organoids embedded in Geltrex in 18-well glass bottom µ-slides (Ibidi, Fräfelfing, Germany) were incubated with different concentrations of H_2O_2 (100,

250, 500, 1000 and 1500 μM) for 10 min. Subsequently, organoids were "redox-fixed" with 10 nM N-ethylmaleimide (NEM) for another 10 min, followed by 15 min of fixation with 2 % PFA. After removal of PFA, organoids were washed with PBS and stored at 4 °C until imaging. Organoids were imaged according to Gutscher et al., 2008, being excited at two different wavelengths (405 nm and 488 nm) [19]. Image analysis was carried out in ImageJ. Organoid outlines were generated by adapting the threshold of the image until the organoid outlines could be defined. Only the mean fluorescent intensities within the organoid outlines were measured.

2.5. Glutathione Analysis

To analyze the levels of oxidized and total glutathione, organoid-derived monolayers were established. To this aim, organoids were released from the Geltrex matrix via repeated pipetting, trypsinized, and resulting single cells were counted. Subsequently, 12,000 cells/well were seeded in 96-well plates pre-coated with 100 μg/mL Geltrex (ThermoFisher Scientific, Vienna, Austria) diluted in basal medium at 37 °C for 1 h. The GSH/GSSG-Glo™ Assay was carried out according to the instructions of the manufacturer (Promega, Madison, WI, USA) for both healthy and IBD-derived monolayers in triplicates once reaching confluence. Cells were stressed with 1000 μM H_2O_2 for 10 min.

2.6. Mitochondrial Stress Analysis

For the analysis of mitochondrial fitness, organoids were incubated with 500 nM MitoTracker® CM-H2Xros for 20 min at 37 °C. Subsequently, organoids were stressed with 1000 μM H_2O_2 to simulate ROS production for 10 min and then fixed with 2 % PFA for another 15 min. After washing with PBS, organoids were stored at 4 °C until confocal imaging. Organoids were analyzed in the same way as ratio images from redox imaging above by outlining the organoids and only analyzing the mean fluorescence intensities of the organoids themselves, excluding any surrounding signal.

2.7. Statistical Analysis

All statistical analyses were performed in Graphpad Prism 10 (GraphPad Software, Boston, MA, USA). *p*-values below 0.05 were considered significant.

3. Results

3.1. Immunofluorescent Analysis

To gain insights into how IBD-derived organoids might be different from healthy patient-derived organoids, we combined DAPI staining with phalloidin to visualize microvilli at the apical cell surface and tight junction staining with Claudin 7. As evidenced by Figure 1, both healthy and IBD-derived organoids present their apical cell surface into the organoid lumen. Additionally, both organoids demonstrate intact tight junctions, i.e., well-structured epithelial barriers.

3.2. Redox Imaging

We used our healthy and IBD-derived organoids, which expressed a redox-sensitive roGFP2-coupled Grx1 protein to analyze the redox balance of the organoids based on the ratio of oxidized to reduced glutathione (GSSG/GSH). The fusion of roGFP2 to glutaredoxin allows for the live cell imaging of the intracellular redox balance since roGFP2 can be excited at two different wavelengths (i.e., 405 nm and 488 nm), depending on its redox state, therefore making ratio calculation possible. After splitting the two acquired image channels and calculating their 405 nm/488 nm ratio, images are presented using the *Fire* filter of ImageJ, which nicely illustrates the resulting ratios with higher values appearing lighter. The results indicate significantly elevated ratios with increasing concentrations of H_2O_2 in both groups. We could observe a slight but significant difference between healthy and IBD-derived organoids (*p*-value 0.0438), showing that in IBD-derived organoids, less glutaredoxin, and hence glutathione, seems to become oxidized (Figure 2A–D).
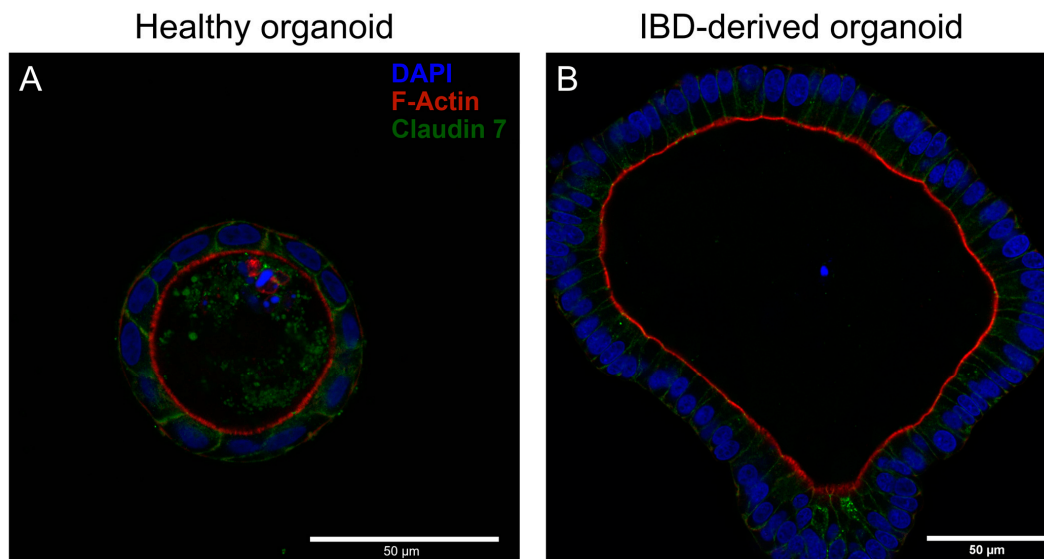
Figure 1. Representative confocal images of Claudin 7/phalloidin/DAPI-stained healthy (**A**) and IBD-derived (**B**) organoids. Both organoids show orientation of phalloidin into the lumen of organoids and well-established cell–cell contacts as evidenced by Claudin 7 staining.
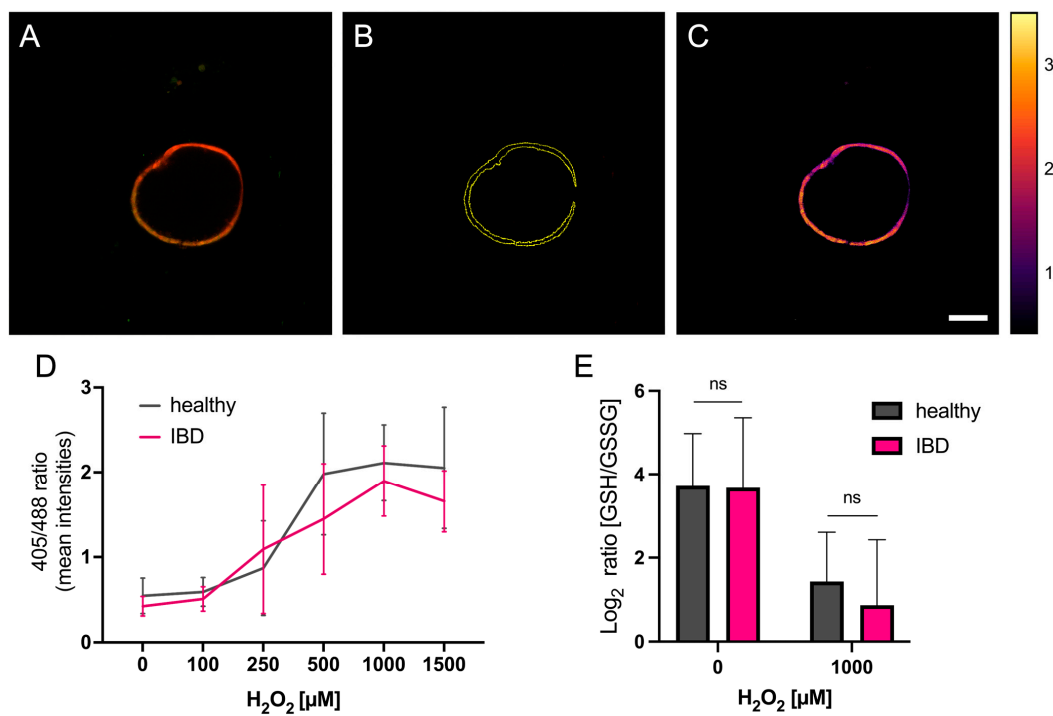

Figure 2. Analysis of ratio imaging with ImageJ. (**A**) Overlay of an exemplary organoid treated with 250 μM H_2O_2 with the two acquired images of both excitation wavelengths (405 nm/488 nm). (**B**) Boundary of the organoid determined by ImageJ. (**C**) Ratio image of the organoid with the *Fire* filter. The boundaries from (**B**) are used to only calculate the ratio of the area of the organoid. Brightness and contrast of (**C**) have been enhanced for visualization purposes only. Scale bar = 100 μm. (**D**) Analysis of ratio imaging from healthy and IBD-derived organoids shows a significant difference between the two organoid lines when increasing H_2O_2 stress treatment (2-way ANOVA: H_2O_2 concentration p-value < 0.0001; health p-value = 0.0438). (**E**) Results from glutathione quantification. GSH/GSSG ratios are not significantly different between healthy and IBD-derived organoid-derived monolayers under both non-stressed and H_2O_2-stressed conditions (Welch t-test). n = three technical replicates including 2–5 evaluated organoids per concentration.

3.3. Glutathione Analysis

To validate the results previously obtained from redox imaging, which only yields a proxy for intracellular glutathione levels and is therefore solely an estimate of the real redox balance, we used a commercial kit to quantify the amount of GSH and GSSG in our samples. These experiments were performed on organoid-derived monolayers (ODM) for standardization reasons, as analyzing a confluent monolayer is easier to define than having the same number of organoids in each well. The results demonstrate that the GSH/GSSG ratios are almost the same in untreated samples. Furthermore, ODMs challenged with H_2O_2 show a clear decrease in the GSH/GSSG ratio. IBD-derived ODMs decrease even further, but not significantly, thus supporting the result from redox imaging (Figure 2E).

3.4. Mitochondrial Stress

Since the mitochondrion is the primary source when it comes to intracellular ROS production, it is crucial to also consider mitochondria when analyzing oxidative stress in organisms. Therefore, we stained active mitochondria in healthy and IBD-derived organoids and looked for differences in stress levels in those samples.

The results clearly demonstrate that cells of both organoid lines appear more stressed after H_2O_2 treatment compared to the untreated controls. With induced oxidative stress, the cells of both organoid lines indicate a higher stress level by increased mean grey values. However, the comparison of both lines demonstrates no significant difference in the level of oxidative stress in the mitochondria (Figure 3).
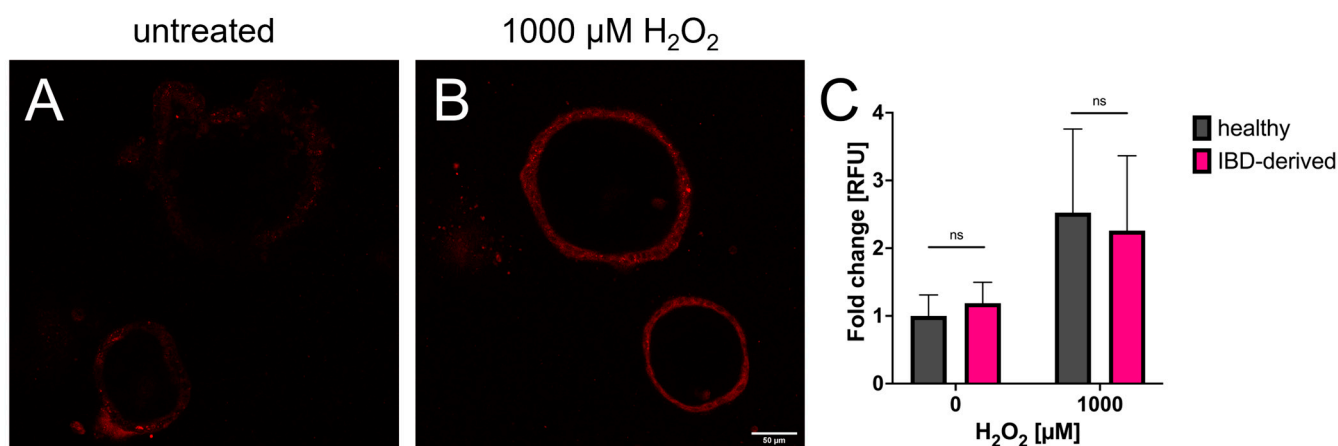

Figure 3. The results from Mitotracker analysis. (**A**,**B**) Representative confocal images of Mitotracker-treated organoids showing the difference between untreated organoids and organoids after being stressed with H_2O_2. Brightness and contrast have been enhanced for visualization purposes only. (**C**) Data from image analysis normalized to untreated healthy organoids. Both healthy and IBD-derived organoids have comparable mitochondrial activity in both stressed and non-stressed conditions (Welch *t*-test). n = three technical replicates including 2–5 evaluated organoids per concentration.

4. Discussion

The aim of this study was to isolate adult stem cells from the duodenum of a healthy dog and one IBD patient to establish a culture of intestinal organoids. Furthermore, we wanted to identify differences between the two organoid samples and test their response to oxidative stress by comparing these two contrary starting conditions.

Several studies have previously analyzed IBD-derived organoids in different regards. For example, d'Aldebert described in 2020 that human IBD-patient-derived organoids present apical-out properties, which means that unlike healthy organoids, IBD-organoids present their apically localized microvilli to the outside. This phenomenon could also be mimicked by incubating healthy organoids with an inflammatory cocktail of three different cytokines (IL-1β, IL-6, TNF-α), which indicates that inflammatory signals are responsible for flipped organoid polarity [20]. However, we could not see that same result in our canine

organoids since both healthy and IBD-derived organoids exhibit proper basal-out polarity with inward-facing microvilli [20]. Other studies focused on the transcriptional profiling of healthy versus IBD-derived organoids and found the overexpression of Paneth cell gene expression in organoids derived from patients with ulcerative colitis (UC) [21] or decreased expression of goblet cell marker gene mucin 2 (*MUC2*) in Crohn's disease patients [22]. These results indicate an atypical apportionment of intestinal cell types that can influence intestinal homeostasis and propagate chronic inflammation. An abnormal distribution of cell types within the intestine can lead to the differential expression of key enzymes responsible for the generation of intracellular ROS including DUOX2 and NOX1, which should be analyzed in future experiments [23].

As mentioned above, intestinal inflammation is accompanied by the production of ROS, which may have further detrimental effects on the healing of lesions and the regeneration of the intestine [9,10,24]. However, there are no reports investigating the role of ROS in IBD-derived organoids in vitro yet. Therefore, we analyzed the antioxidant system of healthy and IBD-derived organoids in several ways to determine whether these organoids have an intrinsically lower antioxidant potential. Furthermore, we show that mitochondrial function is not different between healthy and IBD-derived organoids and is not a probable determinant of chronic intestinal disease.

Our results show only slight differences between IBD-derived and healthy organoids when treated with hydrogen peroxide as a stress inducer. The main purpose was to see how the glutathione ratio changes after stress treatment within different concentrations. The fact that IBD organoids show a significantly lower GSSG/GSH ratio in our ratio imaging approach is interesting and unexpected, as IBD organoids were expected to be more sensitive to redox stress compared to healthy organoids. It is tempting to speculate that IBD-derived organoids might possess upregulated basal levels of glutaredoxin expression to cope with increased levels of ROS in vivo.

The results from the GSH/GSSG assays correlate well with the results obtained from ratio imaging. While an increase in ratio up to about 2-fold could be measured in ratio imaging with increasing concentrations of H_2O_2, GSH/GSSG assays show a greater than 2-fold reduction compared to oxidized glutathione. As the ratios are calculated reversely, both assays show the same result. Therefore, both systems are well-suited for redox analysis. Nevertheless, we could not observe a shift towards more glutathione in IBD-derived organoids.

We would like to point out that the concentrations of H_2O_2 in our assays are likely beyond physiological levels [25]. However, concentrations up to 1.5 mM have previously been used in combinations with the same Grx1-roGFP2 sensor to analyze the antioxidant system of cells [16]. Since we attempted to analyze the organoids' ability to absorb the shock of being stressed, we used higher levels of hydrogen peroxide to analyze the full potential to eradicate ROS. Higher levels of H_2O_2 may also be necessary to achieve quick diffusion through the extracellular matrix (ECM) that will differ from analysis on cells without them being embedded in the ECM [26].

5. Conclusions

In summary, our results indicate neither a drastically imbalanced antioxidant system in IBD-derived organoids nor a malfunction of mitochondria. Despite these results, the redox system should not be ruled out entirely as a factor contributing to IBD, as our IBD-derived organoids behave differently upon H_2O_2 challenge compared to healthy organoids in ratio imaging. Many other parameters in vivo may influence redox balance that remain to be modelled in vitro in future studies. These include the incorporation of other cell types like fibroblasts, endothelial cells, and immune cells into three-dimensional organoid cultures.

In 2015, co-culturing intestinal organoids with lamina propria lymphocytes showed an increased size of organoids, elevated intestinal stem cell regeneration and proliferation dependent on IL-22. In addition, the introduction of monocyte-derived macrophages and an infection via *E. coli* in human colon organoids led to an altered macrophage morphology,

increased migration, cytokine secretion and mirrored inflammatory bowel disease [27]. However, co-cultures with immune cells are still not state of the art in organoid research as it makes intestinal organoid cultures much more complex and more difficult to analyze but could also help to elucidate miniscule differences between healthy and IBD-derived organoids that may have relevant overall effects.

Nonetheless, our study relied on a very small sample size and should be validated with a higher number of organoids derived from different patients as our results are still very preliminary. Additionally, the process of inflammation could be different between canines and humans, which might explain the difference in organoid polarity compared to d'Aldebert et al., 2020. One more reason for the lack of differences between healthy and IBD-derived samples can be the difficulty in the diagnosis of IBD itself. There are multiple symptoms of the disease, which can overlap with symptoms of various other illnesses (e.g., variable stool consistency and frequency) [28].

However, the advancement of this organoid model system may offer a promising approach to promote the goals of One Health and help to further reduce animal testing and optimize animal welfare in the world of science.

Author Contributions: Conceptualization, G.C.; methodology, G.C., J.H. and S.T.; formal analysis, G.C. and J.H.; investigation, G.C., J.H. and S.T.; data curation, G.C. and J.H.; writing—original draft preparation, G.C. and J.H.; writing—review and editing, G.C., J.H., S.T., B.P. and I.A.B.; visualization, G.C. and J.H.; supervision, G.C., B.P. and I.A.B.; project administration, G.C.; funding acquisition, G.C., S.T. and I.A.B. All authors have read and agreed to the published version of the manuscript.

Institutional Review Board Statement: Not applicable.

Informed Consent Statement: Not applicable.

Data Availability Statement: The raw data supporting the conclusions of this article will be made available by the authors upon inquiry.

Conflicts of Interest: The authors declare no conflict of interest. The funders had no role in the design of the study; in the collection, analyses, or interpretation of data; in the writing of the manuscript; or in the decision to publish the results.

References

1. Günther, C.; Winner, B.; Neurath, M.F.; Stappenbeck, T.S. Organoids in Gastrointestinal Diseases: From Experimental Models to Clinical Translation. *Gut* **2022**, *71*, 1892–1908. [CrossRef]
2. Dutta, D.; Clevers, H. Organoid Culture Systems to Study Host–Pathogen Interactions. *Curr. Opin. Immunol.* **2017**, *48*, 15–22. [CrossRef]
3. Csukovich, G.; Pratscher, B.; Burgener, I.A. The World of Organoids: Gastrointestinal Disease Modelling in the Age of 3R and One Health with Specific Relevance to Dogs and Cats. *Animals* **2022**, *12*, 2461. [CrossRef] [PubMed]
4. Stange, E.F. Current and Future Aspects of IBD Research and Treatment: The 2022 Perspective. *Front. Gastroenterol.* **2022**, *1*, 914371. [CrossRef]
5. Soontararak, S.; Chow, L.; Johnson, V.; Coy, J.; Webb, C.; Wennogle, S.; Dow, S. Humoral Immune Responses against Gut Bacteria in Dogs with Inflammatory Bowel Disease. *PLoS ONE* **2019**, *14*, e0220522. [CrossRef]
6. Jiminez, J.A.; Uwiera, T.C.; Inglis, G.D.; Uwiera, R.R.E. Animal Models to Study Acute and Chronic Intestinal Inflammation in Mammals. *Gut. Pathog* **2015**, *7*, 29. [CrossRef] [PubMed]
7. Craven, M.; Simpson, J.W.; Ridyard, A.E.; Chandler, M.L. Canine Inflammatory Bowel Disease: Retrospective Analysis of Diagnosis and Outcome in 80 Cases (1995–2002). *J. Small Anim. Pract.* **2004**, *45*, 336–342. [CrossRef]

8.   Washabau, R.J.; Day, M.J.; Willard, M.D.; Hall, E.J.; Jergens, A.E.; Mansell, J.; Minami, T.; Bilzer, T.W. Endoscopic, Biopsy, and Histopathologic Guidelines for the Evaluation of Gastrointestinal Inflammation in Companion Animals. *J. Vet. Intern. Med.* **2010**, *24*, 10–26. [CrossRef]

9.   Singh, V.; Ahlawat, S.; Mohan, H.; Gill, S.S.; Sharma, K.K. Balancing Reactive Oxygen Species Generation by Rebooting Gut Microbiota. *J. Appl. Microbiol.* **2022**, *132*, 4112–4129. [CrossRef]

10.   Tian, T.; Wang, Z.; Zhang, J. Pathomechanisms of Oxidative Stress in Inflammatory Bowel Disease and Potential Antioxidant Therapies. *Oxidative Med. Cell. Longev.* **2017**, *2017*, 4535194. [CrossRef]

11.   Bourgonje, A.R.; Feelisch, M.; Faber, K.N.; Pasch, A.; Dijkstra, G.; van Goor, H. Oxidative Stress and Redox-Modulating Therapeutics in Inflammatory Bowel Disease. *Trends Mol. Med.* **2020**, *26*, 1034–1046. [CrossRef]

12.   Cao, Z.; Lindsay, J.G.; Isaacs, N.W. Mitochondrial Peroxiredoxins: Structure and Function. *Subcell. Biochem.* **2007**, *44*, 295–315. [CrossRef] [PubMed]

13.   Zhao, M.; Wang, Y.; Li, L.; Liu, S.; Wang, C.; Yuan, Y.; Yang, G.; Chen, Y.; Cheng, J.; Lu, Y.; et al. Mitochondrial ROS Promote Mitochondrial Dysfunction and Inflammation in Ischemic Acute Kidney Injury by Disrupting TFAM-Mediated MtDNA Maintenance. *Theranostics* **2021**, *11*, 1845. [CrossRef]

14.   Lv, H.; Zhen, C.; Liu, J.; Yang, P.; Hu, L.; Shang, P. Unraveling the Potential Role of Glutathione in Multiple Forms of Cell Death in Cancer Therapy. *Oxid. Med. Cell. Longev.* **2019**, *2019*, 3150145. [CrossRef]

15.   Forman, H.J.; Zhang, H.; Rinna, A. Glutathione: Overview of Its Protective Roles, Measurement, and Biosynthesis. *Mol. Asp. Med.* **2009**, *30*, 1–12. [CrossRef] [PubMed]

16.   Hatori, Y.; Kubo, T.; Sato, Y.; Inouye, S.; Akagi, R.; Seyama, T. Visualization of the Redox Status of Cytosolic Glutathione Using the Organelle-and Cytoskeleton-Targeted Redox Sensors. *Antioxidants* **2020**, *9*, 129. [CrossRef] [PubMed]

17.   Kramer, N.; Pratscher, B.; Meneses, A.M.C.; Tschulenk, W.; Walter, I.; Swoboda, A.; Kruitwagen, H.S.; Schneeberger, K.; Penning, L.C.; Spee, B.; et al. Generation of Differentiating and Long-Living Intestinal Organoids Reflecting the Cellular Diversity of Canine Intestine. *Cells* **2020**, *9*, 822. [CrossRef]

18.   van Ineveld, R.L.; Ariese, H.C.R.; Wehrens, E.J.; Dekkers, J.F.; Rios, A.C. Single-Cell Resolution Three-Dimensional Imaging of Intact Organoids. *J. Vis. Exp.* **2020**, *2020*, e60709. [CrossRef]

19.   Gutscher, M.; Pauleau, A.L.; Marty, L.; Brach, T.; Wabnitz, G.H.; Samstag, Y.; Meyer, A.J.; Dick, T.P. Real-Time Imaging of the Intracellular Glutathione Redox Potential. *Nat. Methods* **2008**, *5*, 553–559. [CrossRef] [PubMed]

20.   d'Aldebert, E.; Quaranta, M.; Sébert, M.; Bonnet, D.; Kirzin, S.; Portier, G.; Duffas, J.P.; Chabot, S.; Lluel, P.; Allart, S.; et al. Characterization of Human Colon Organoids from Inflammatory Bowel Disease Patients. *Front. Cell Dev. Biol.* **2020**, *8*, 363. [CrossRef]

21.   Dotti, I.; Mora-Buch, R.; Ferrer-Picón, E.; Planell, N.; Jung, P.; Masamunt, M.C.; Leal, R.F.; de Carpi, J.M.; Llach, J.; Ordás, I.; et al. Alterations in the Epithelial Stem Cell Compartment Could Contribute to Permanent Changes in the Mucosa of Patients with Ulcerative Colitis. *Gut* **2017**, *66*, 2069–2079. [CrossRef] [PubMed]

22.   Noben, M.; Verstockt, B.; de Bruyn, M.; Hendriks, N.; Van Assche, G.; Vermeire, S.; Verfaillie, C.; Ferrante, M. Epithelial Organoid Cultures from Patients with Ulcerative Colitis and Crohns Disease: A Truly Long-Term Model to Study the Molecular Basis for Inflammatory Bowel Disease? *Gut* **2017**, *66*, 2193–2195. [CrossRef]

23.   Stenke, E.; Bourke, B.; Knaus, U.G. NAPDH Oxidases in Inflammatory Bowel Disease. In *Methods in Molecular Biology*; Springer Nature: Cham, Switzerland, 2019; Volume 1982.

24.   Zhou, G.; Yu, L.; Fang, L.; Yang, W.; Yu, T.; Miao, Y.; Chen, M.; Wu, K.; Chen, F.; Cong, Y.; et al. CD177+ Neutrophils as Functionally Activated Neutrophils Negatively Regulate IBD. *Gut* **2018**, *67*, 1052–1063. [CrossRef] [PubMed]

25.   Sies, H. Hydrogen Peroxide as a Central Redox Signaling Molecule in Physiological Oxidative Stress: Oxidative Eustress. *Redox Biol.* **2017**, *11*, 613–619. [CrossRef]

26.   Lim, J.B.; Langford, T.F.; Huang, B.K.; Deen, W.M.; Sikes, H.D. A Reaction-Diffusion Model of Cytosolic Hydrogen Peroxide. *Free Radic. Biol. Med.* **2016**, *90*, 85–90. [CrossRef] [PubMed]

27.   Yip, S.; Wang, N.; Sugimura, R. Give Them Vasculature and Immune Cells—How to Fill the Gap of Organoids. *Cells Tissues Organs* **2023**, 1–14. [CrossRef] [PubMed]

28.   Allenspach, K.; Wieland, B.; Gröne, A.; Gaschen, F. Chronic Enteropathies in Dogs: Evaluation of Risk Factors for Negative Outcome. *J. Vet. Intern. Med.* **2007**, *21*, 700–708. [CrossRef]